The Intracellular Transport of Low Density Lipoprotein-derived Cholesterol Is Defective in Niemann-Pick Type C Fibroblasts

Laura Liscum, Regina M. Ruggiero, and Jerry R. Faust

Department of Physiology, Tufts University School of Medicine, Boston, Massachusetts 02111

Abstract. Niemann-Pick disease type C (NPC) is characterized by substantial intracellular accumulation of unesterified cholesterol. The accumulation of unesterified cholesterol in NPC fibroblasts cultured with low density lipoprotein (LDL) appears to result from the inability of LDL to stimulate cholesterol esterification in addition to impaired LDL-mediated downregulation of LDL receptor activity and cellular cholesterol synthesis. Although a defect in cholesterol transport in NPC cells has been inferred from previous studies, no experiments have been reported that measure the intracellular movement of LDL-cholesterol specifically. We have used four approaches to assess intracellular cholesterol transport in normal and NPC cells and have determined the following: (*a*) mevinolin-inhibited NPC cells are defective in using LDL-cholesterol for growth. However, exogenously added mevalonate restores cell growth equally in normal and NPC cells; (*b*) the transport of LDL-derived [^{3}H]cholesterol to the plasma membrane is slower in NPC cells, while the rate of appearance of [^{3}H]acetate-derived, endogenously synthesized [^{3}H]cholesterol at the plasma membrane is the same for normal and NPC cells; (*c*) in NPC cells, LDL-derived [^{3}H]cholesterol accumulates in lysosomes to higher levels than normal, resulting in defective movement to other cell membranes; and (*d*) incubation of cells with LDL causes an increase in cholesterol content of NPC lysosomes that is threefold greater than that observed in normal lysosomes. Our results indicate that a cholesterol transport defect exists in NPC that is specific for LDL-derived cholesterol.

MAMMALIAN cells require cholesterol for growth. When cultured in the presence of serum, cells acquire cholesterol by receptor-mediated endocytosis of low density lipoprotein (LDL)[1] (8). LDL is delivered to lysosomes where the protein/phospholipid coat is degraded, and LDL-cholesteryl esters are hydrolyzed to unesterified cholesterol. LDL-derived cholesterol is used by cells to synthesize cellular membranes, bile acids, and steroid hormones (8). LDL-derived cholesterol also elicits several regulatory responses, including suppression of cholesterol biosynthesis and LDL receptor activity, as well as activation of the cholesterol-esterifying enzyme, acyl coenzyme A/cholesterol acyl transferase (ACAT) (8). The process of receptor-mediated internalization of LDL and the effects of LDL-cholesterol on cellular cholesterol metabolism have been extensively studied (8); however, little information is known about the fate of cholesterol formed by lysosomal hydrolysis of LDL-cholesteryl esters. In particular, the pathway and mechanism of intracellular transport of LDL-cholesterol from lysosomes to cellular membranes are obscure. In addition, it is not known whether the regulatory actions of LDL-cholesterol require either the transport of cholesterol to regulatory sites within cells or metabolic transformation of the sterol.

Somatic cells exhibiting specific defects in LDL metabolism may be useful in delineating the mechanisms of intracellular transport of and regulation by LDL-cholesterol. A defect in LDL-cholesterol metabolism in fibroblasts from patients with Niemann-Pick disease type C (NPC) has been described by Pentchev and co-workers (25–27) and our laboratory (21). Although LDL is bound and internalized, and the cholesteryl esters hydrolyzed normally in NPC fibroblasts, LDL-derived cholesterol does not elicit normal regulatory responses (21, 25–27). In NPC cells, LDL does not stimulate cholesterol esterification, and LDL suppression of cholesterol synthesis and LDL receptor activity is impaired (21, 25, 27). The defective regulation of cellular cholesterol metabolism in NPC cells appears to be specific for LDL-derived cholesterol, since 25-hydroxycholesterol, a nonlipoprotein effector, does stimulate cholesterol esterification as well as downregulate cholesterol synthesis and LDL receptor activity normally in NPC cells (21). Also, exogenously added mevalonate suppresses cholesterol synthesis equally well in normal and NPC cells (21).

One possible explanation for the lack of LDL-mediated regulation of cholesterol metabolism in NPC cells is that the intracellular transport of cholesterol is defective (21, 27, 32).

1. *Abbreviations used in this paper*: ACAT, acyl coenzyme A/cholesterol acyl transferase; LDL, low density lipoprotein; [^{3}H-CL]LDL, LDL labeled with [^{3}H]cholesteryl linoleate; *N*Aβ*G*, *N*-acetyl-β-D-glucosaminidase; NPA, Niemann-Pick disease type A; NPC, Niemann-Pick disease type C; SUV, small unilamellar vesicle.

In the current study, four approaches were used to examine cholesterol transport in normal and NPC fibroblasts. We have measured (*a*) the ability of LDL-derived and endogenously synthesized cholesterol to support cell growth; (*b*) the intracellular movement of LDL-derived and endogenously synthesized cholesterol; (*c*) the transfer of LDL-derived cholesterol from lysosomes to other cell membranes; and (*d*) cholesterol content of lysosomes and cell membranes from cells incubated with LDL.

We found that the movement of LDL-derived cholesterol from lysosomes to other cell membranes is impaired in NPC cells, while the movement of endogenously synthesized cholesterol is normal. The finding that NPC fibroblasts express a defect in LDL-derived cholesterol transport provides us with a valuable tool with which to study intracellular cholesterol movement.

Materials and Methods

[1,2,6,7-^{3}H]Cholesteryl linoleate (97.1 Ci/mmol), [4-^{14}C]cholesterol (53.2 mCi/mmol), and sodium [^{3}H]acetate (100 mCi/mmol) were purchased from DuPont-New England Nuclear (Boston, MA). Mevinolin was a gift of A. Alberts, Merck Research Laboratory (Rahway, NJ). M. Krieger, Biology Department, Massachusetts Institute of Technology, generously supplied us with human lipoprotein-deficient serum and LDL. A specific inhibitor of ACAT, 58-035 (3-[decyldimethylsilyl]-*N*-[2-(4-methylphenyl)-1-phenylethyl]propanamide), was provided by Sandoz Inc. (E. Hanover, NJ). Percoll was obtained from Pharmacia Fine Chemicals (Piscataway, NJ). Cholesterol (recrystallized from ethanol three times before use) and stigmasterol were obtained from Steraloids, Inc. (Wilton, NH). L-α-phosphatidylcholine from fresh egg yolk and all other reagents were from Sigma Chemical Co. (St. Louis, MO) or obtained as previously described (21).

Preparation of LDL, Lipoprotein-Deficient Serum, and LDL Labeled with [^{3}H]Cholesteryl Linoleate ([^{3}H-CL]LDL)

LDL was prepared by ultracentrifugation (16). Fetal bovine lipoprotein-deficient serum was prepared from FBS omitting the thrombin incubation (16). [^{3}H-CL]LDL was prepared with an average specific activity of 18,400 cpm/nmol of total cholesteryl linoleate in LDL (13).

Preparation of Media and Buffers

The following media were prepared: medium A (MEM supplemented with 10% [vol/vol] FBS, 2 mM glutamine, 100 units/ml penicillin, 100 μg/ml streptomycin, 1% [vol/vol] each of essential amino acids, nonessential amino acids and vitamins, and 20 mM Hepes, pH 7.3); medium B (medium A in which 10% [vol/vol] FBS is replaced with 10% [vol/vol] fetal bovine lipoprotein-deficient serum); and medium C (medium A in which 10% [vol/vol] FBS is replaced with 10% [vol/vol] human lipoprotein-deficient serum).

The following buffers were prepared: buffer A (150 mM NaCl, 50 mM Tris-chloride, pH 7.4); buffer B (buffer A containing 2 mg/ml BSA); and buffer C (250 mM sucrose, 1 mM EDTA).

Cultured Cells

Normal (GM 5659), NPC (GM 3123), and Niemann-Pick type A (NPA) (GM 0112) fibroblasts were obtained from the Human Mutant Cell Repository (Camden, NJ) and grown as described previously (21) in medium A. Experiments were carried out using one of three formats.

Format 1. On day 0, cells were seeded into 12-well plates (5,000 cells/22.6-mm well) in 1 ml of medium B.

Format 2. On day 0, cells were seeded into 6-well plates (40,000 cells/35 mm well) in 1.5 ml of medium B. On day 2, medium was replaced with 1 ml of medium B.

Format 3. On day 0, cells were seeded into 150-mm dishes (200,000–300,000 cells/dish) in 15 ml of medium A. On day 2 or 3, monolayers were washed with 15 ml of Earle's balanced salt solution and refed with 15 ml of medium B.

Cell Growth

Cells were grown according to Format 1. On day 1, monolayers were refed with 1.5 ml of medium B or medium B containing 20 μM mevinolin, 0.15 mM mevalonate plus various amounts of LDL or additional mevalonate. At the same time, 1.5 ml of medium B was added to each well of another 12-well plate containing no cells in which a BSA standard curve was performed during the Lowry determination. On day 8, wells were washed once quickly, three times (10 min, 20°C), and once quickly with buffer A. The residual liquid in the wells was completely aspirated, and additions of BSA (0–30 μg) were made to wells of the "no cell/standard curve" plate. Cell-associated protein was dissolved with 1 ml of Lowry reagent. Protein was measured directly in the wells by the Lowry method (22). Cell growth is expressed as microgram of cell protein per well.

Movement of Cholesterol to the Plasma Membrane

To prepare small unilamellar vesicles (SUV) cholesterol (160 μmol) and L-α-phosphatidylcholine (232 μmol) were dried (37°C, N_2) and lyophilized (2). The lipid sample was dispersed in 4 ml of PBS and sonicated (1 h, 4°C) under N_2 using a sonifier at setting 3 (model 185; Branson Sonic Power Co., Danbury, CT). The dispersion was centrifuged (12,000 *g*, 5 min) to remove titanium that was shed by the probe, stored at 4°C, and used within 3 d.

Cells were grown according to format 2. On day 4, monolayers were refed 1 ml of either (*a*) medium C plus 20 μM mevinolin, 1 μg/ml 58-035, and 30 μg/ml [^{3}H-CL]LDL, or (*b*) medium C containing 15 μCi/ml [^{3}H]acetate. LDL will stimulate cholesterol esterification in normal, but not NPC cells (21, 25). To negate any differential effect that cholesterol esterification may have on intracellular transport of LDL-cholesterol within the two cell lines, ACAT was inhibited in both cell types by the addition of 58-035. Similarly, mevinolin was included to negate unequal LDL-mediated suppression of cholesterol synthesis in normal and NPC cells (21). After 2 h, monolayers were washed with 3 ml of Earle's balanced salt solution and refed with 1 ml of medium C plus 50 μl SUVs (containing 2 μmol cholesterol and 2.9 μmol L-α-phosphatidylcholine).

Cells were harvested at staggered times. Media were removed and centrifuged (12,000 *g*, 5 min, 4°C). Ethanol (1 ml) was added to media from cells incubated with [^{3}H-CL]LDL. Media from [^{3}H]acetate-labeled cells were saponified to facilitate the separation of [^{3}H]cholesterol from other [^{3}H]acetate-derived products. Each sample received 1 ml of 25% (wt/vol) KOH in ethanol and was heated (80°C, 1 h). All media samples were then extracted twice with 2 ml of petroleum ether. Pooled petroleum ether extracts were backwashed with 1 ml of water, and evaporated to dryness. [^{3}H]Cholesterol and [^{3}H]cholesteryl ester were separated by TLC using toluene/ethyl acetate (2:1) for [^{3}H-CL]LDL-labeled samples and heptane/ethyl ether (95:55) for [^{3}H]acetate-labeled samples.

Cell monolayers were washed once quickly, two times (7 min, 4°C) with 3 ml of buffer B, and two times quickly with buffer A. All monolayers were extracted with hexane/isopropyl alcohol (3:2). The [^{3}H-CL]LDL-labeled cell extracts were subjected to TLC (21). [^{3}H]Acetate-labeled cell extracts were saponified, extracted, and subsequently subjected to TLC as described above for the media samples. Cellular protein on the dishes was dissolved in 0.1 N NaOH, and an aliquot taken for Lowry protein determination (22).

[^{3}H]Cholesteryl ester and [^{3}H]cholesterol content are expressed as nmol/mg cell protein or pmol/mg cell protein for [^{3}H-CL]LDL and [^{3}H]-acetate-labeled cells, respectively. The endogenously synthesized [^{3}H]sterol was identified as [^{3}H]cholesterol by cochromatography with [^{14}C]cholesterol and authentic unlabeled cholesterol. [^{14}C]Cholesterol (2,000 cpm, 40 μg) and cholesteryl oleate (20 μg) were added as chromatography standards and to correct for procedural losses (averaging 35%).

Percoll Gradient Fractionation of [^{3}H-CL]LDL-labeled Fibroblasts

Cells were grown according to format 3. On day 4 or 5, monolayers were incubated with [^{3}H-CL]LDL in 15 ml of medium C.

Pulse-chase Protocol (Figs. 4–7). At staggered times, cells were pulse labeled with 5 μg/ml [^{3}H-CL]LDL for 1 h. The monolayers were then washed twice quickly (20°C) with 15 ml of Earle's balanced salt solution containing 20 mg/ml BSA, refed with 15 ml of medium C, and replaced in the CO_2 incubator for various chase times.

Continuous Label Protocol (Fig. 8). Additions of 2 μg/ml [^{3}H-CL]-LDL were made at staggered times.

All dishes were harvested at the same time. Media were removed and

lyophilized in 50-ml glass tubes. The dried media samples were dissolved in 4 ml of water followed by 4 ml of ethanol and extracted twice with 8 ml of petroleum ether. The combined petroleum ether extracts were backwashed with 2 ml of water and evaporated to dryness. [^{3}H]Cholesterol and [^{3}H]cholesteryl ester were isolated by TLC using toluene/ethyl acetate (2:1). The monolayers were washed once quickly and once (7 min, 4°C) with 15 ml of buffer B, once (7 min, 4°C) with 15 ml of buffer A, then once quickly and once (7 min, 4°C) with 15 ml buffer C. Cells were scraped, pelleted by centrifugation (2000 *g*, 5 min, 4°C), disrupted in 1 ml of buffer C by 2 strokes in a 2-ml tight-fitting Dounce tissue grinder (Kontes Co., Vineland, NJ). The homogenates were centrifuged (2000 *g*, 5 min, 4°C), and the pellets were resuspended in buffer C (600 μl), rehomogenized, and centrifuged again. The 2,000-*g* pellets were resuspended in buffer C (600 μl). The resulting postnuclear supernatants were combined (1.5 ml total), and 1 ml (100–180 μg total cell protein) was layered onto 9 ml of 7.8% (vol/vol) Percoll in buffer C. Gradients were subjected to centrifugation (20,000 *g*, 40 min, 4°C) in a rotor, (model Ti50, Beckman Instruments, Inc., Palo Alto, CA) then fractionated into 10 equal portions. A reference gradient was developed simultaneously by loading 1 ml of buffer C onto 9 ml of 7.8% Percoll and centrifuging with the samples.

Cell Fractionation Assays

Aliquots (200–500 μl) of postnuclear supernatants, 2,000-*g* pellets, and gradient fractions were assayed for [^{3}H]cholesteryl ester and [^{3}H]cholesterol content following Bligh and Dyer extraction (5). To facilitate phase separation, additional $CHCl_3$ (1.5 vol) and water (1.5 vol) were added to gradient samples that contained high concentrations of Percoll. Following centrifugation, the organic phases were dried with air, and [^{3}H]cholesterol and [^{3}H]cholesteryl ester were separated by TLC using toluene/ethyl acetate (2:1). [^{3}H]Cholesteryl ester and [^{3}H]cholesterol content in the cells (sum of postnuclear supernatant and 2,000-*g* pellet) and media are expressed as nmol/mg protein. [^{3}H]Cholesterol content in the gradient fractions are expressed as pmol/fraction. [^{14}C]Cholesterol (2,000 cpm, 40 μg) and cholesteryl oleate (20 μg) were added at the time of extraction as chromatography standards and to correct for procedural losses (averaging 26%). Protein was measured in postnuclear supernatants and 2,000-*g* pellets by a Lowry assay (22). Densities of gradient fractions derived from a reference Percoll gradient were measured with a refractometer (Bausch & Lomb Inc., Rochester, NY).

N-acetyl-β-glucosaminidase (*NA*β*G*) activity was measured in 49 mM sodium citrate, pH 4.5, 77 mM KCl, 0.033% (vol/vol) Triton X-100 with 2.4 mM *p*-nitrophenyl *N*-acetyl-β-D-glucosaminide in a final volume of 750 μl (3). After 30 min at 37°C, the reaction was stopped by the addition of 500 μl of 0.4 M glycine, pH 10.4. The absorbance of released *p*-nitrophenol was measured at 420 nm and compared to the absorbance of *p*-nitrophenol standards (5–100 nmol). Parallel incubations were performed with aliquots of the reference (no cell extract) gradient fractions, and the absorbance due to Percoll was subtracted from the experimental values. One unit of *NA*β*G* activity represents the formation of 1 nmol of *p*-nitrophenol/30 min.

5′ nucleotidase activity was measured in 36 mM Tris, pH 8.5, 8 mM $MgCl_2$, 0.10% (vol/vol) Triton X-100, and 2.3 mM 5′-AMP in a final volume of 1 ml (36). After 60 min at 37°C, 200 μl of 30% TCA was added, and the samples were centrifuged (12,000 *g*, 5 min). An aliquot (400 μl) of the supernatant was added to 1 ml of Ames reagent (1). After 60 min at 37°C, the absorbance at 820 nm was determined. Liberated P_i was quantitated with standards (2.5–40 nmol) that were reacted with the Ames reagent. One unit of 5′-nucleotidase activity represents the formation of 1 nmol of P_i/60 min.

Cholesterol Content of Subcellular Fractions

Cells were grown according to format 3. Monolayers were harvested according to the procedure for Percoll gradient fractionation (see above) except that dishes were washed 3 × 7 min with buffer B. Cell pellets derived from two 150-mm dishes were pooled before the Dounce homogenization. Percoll gradient fractions displaying the highest 5′ nucleotidase (fractions 3–5) and *NA*β*G* (fractions 9–10) activities were pooled to obtain light membranes and lysosomes, respectively, and centrifuged (100,000 *g*, 90 min) to pellet the Percoll (methodology booklet No. 19, Pharmacia Fine Chemicals). Aliquots of the light membrane and lysosome supernatants were lyophilized and subjected to Folch extraction (15). Aliquots of postnuclear supernatants were Folch-extracted directly. The unesterified cholesterol content was determined after separation by gas–liquid chromatography using a 3% OV-17 on 80/100 Gas Chrom Q column (6 feet by 0.085 inch, internal diameter) (Alltech Associates, Inc., Deerfield, IL) and quantitated using a flame ionization detector. Stigmasterol was added to each sample before the Folch extraction as an internal standard. Aliquots of the postnuclear supernatants were taken for measurement of protein, 5′ nucleotidase activity, *NA*β*G* activity, and cholesterol content. Aliquots of light membrane and lysosome supernatant were taken for measurement of 5′ nucleotidase and *NA*β*G* activities, respectively, and cholesterol content. The specific activities of *NA*β*G* and 5′ nucleotidase were the same in postnuclear supernatants of normal and NPC cells incubated in the absence and presence of LDL (see Table I).

Table I. LDL-induced Increase in Cholesterol Content of Postnuclear Supernatants and Lysosomal and Light Membrane Percoll Gradient Fractions from Normal and NPC Cells

	Normal Cells			NPC Cells		
	−LDL (*a*)	+LDL (*b*)	Fold increase (*b/a*)	−LDL (*a*)	+LDL (*b*)	Fold increase (*b/a*)
Postnuclear supernatants						
Protein (μg)	365	368		567	494	
5′ Nucleotidase activity (U/μg)	19.3	18.2		17.5	17.3	
*NA*β*G* activity (U/μg)	12.0	10.4		11.2	9.6	
Cholesterol (pmol/μg)	110	240	2.2	110	400	3.6
Light Membranes						
5′ Nucleotidase activity (U)	1,608	2,043		1,995	1,981	
Cholesterol (pmol/U 5′ nucleotidase activity)	2.6	8.5	3.3	3.9	13.7	3.5
Lysosomes						
*NA*β*G* activity (U)	918	842		2,077	1,044	
Cholesterol (pmol/U *NA*β*G* activity)	8.5	18.4	2.2	5.9	41.7	7.1

Cells were grown according to format 3. On day 3, monolayers were refed 15 ml of medium C (−LDL) or medium C plus 25 μg/ml LDL (+LDL). Cells were harvested after 14 h. Percoll gradient fractionation of normal and NPC postnuclear supernatants was carried out as described in Materials and Methods. The cholesterol content of postnuclear supernatants, lysosome, and light membrane Percoll gradient fractions was determined by gas–liquid chromatography as described in Materials and Methods. Protein content, *NA*β*G* and 5′ nucleotidase activities of postnuclear supernatants, and light membrane and lysosomal Percoll gradient fractions were determined as described in Materials and Methods. The fold increase (*b/a*) represents the ratio of the cholesterol content in +LDL (*b*) and −LDL (*a*) samples.

Results

LDL- and Mevalonate-dependent Growth of Normal and NPC Fibroblasts

Mammalian cells require an exogenous source of cholesterol when cultured in the presence of mevinolin, an inhibitor of mevalonate synthesis, and thus, cholesterol biosynthesis (7, 24). The ability of LDL-derived cholesterol to reverse mevinolin-inhibited cell growth was examined in normal and NPC fibroblasts (Fig. 1 *A*). Cell monolayers were grown in medium B or medium B containing 20 μM mevinolin, 0.15 mM mevalonate, and varying concentrations of LDL (Fig. 1 *A*). Mevalonate, at 0.15 mM, is sufficient to supply essential nonsterol isoprenoid products (such as ubiquinone and dolichol), but the low concentration of mevalonate is not converted to cholesterol in sufficient amounts to support the sterol requirements of the cells (7, 12, 14). After 8 d, the protein content of the wells was measured as an indication of cell growth.

The protein content in wells of normal fibroblasts cultured in medium B was 44 μg/well. When normal fibroblasts were cultured in medium B containing 20 μM mevinolin and 0.15 mM mevalonate, growth was inhibited, and the wells contained 0.2 μg of protein. The addition of LDL to mevinolin-inhibited cells increased cell growth in a concentration-dependent manner; normal cells cultured with mevinolin plus 2.5–3.1 μg/ml LDL grew to the same level as uninhibited cells (Fig. 1 *A*). The protein content in wells of NPC fibroblasts grown in medium B and medium B containing 20 μM mevinolin and 0.15 mM mevalonate was 43 and 0.5 μg of protein per well, respectively. Although uninhibited growth rates were the same for both cell types, LDL-cholesterol was less effective at reversing the mevinolin-inhibited growth of NPC cells.

Cultured mammalian cells will also grow in the presence of mevinolin if supplied with high concentrations of exogenous mevalonate (24). Mevalonate is taken up by cells and used as substrate for de novo cholesterol synthesis. Monolayers were cultured in medium B or medium B containing 20 μM mevinolin and varying concentrations of mevalonate (Fig. 1 *B*). We observed that mevalonate restored cell growth equally in normal and NPC fibroblasts. This result indicates that newly synthesized cholesterol is capable of supporting the growth of normal and NPC cells equally.

Movement of LDL-derived and Endogenously Synthesized Cholesterol to the Plasma Membrane in Normal and NPC Cells

The intracellular transport of LDL-derived [^{3}H]cholesterol from lysosomes to plasma membranes was examined using [^{3}H-CL]LDL (13). [^{3}H-CL]LDL binds to the LDL receptor and is internalized and delivered to lysosomes where hydrolysis releases [^{3}H]cholesterol. We documented the time course of movement of LDL-derived [^{3}H]cholesterol from lysosomes to plasma membranes by determining the amount of [^{3}H]cholesterol that desorbs from the cells and appears in the media during chase incubations. Chase incubations were performed in media containing SUVs to insure an adequate trap for the desorbed cellular [^{3}H]cholesterol (10, 28, 30).

The appearance of [^{3}H]cholesterol in the media is most likely the result of either the desorption of plasma membrane [^{3}H]cholesterol and its trapping by phospholipid vesicles in the medium, or the secretion of lysosomal contents. Evidence that supports the former is as follows. First, the appearance of both LDL-derived and endogenously sythesized [^{3}H]cholesterol in the medium was dependent upon the presence of phospholipid vesicles. Control experiments were performed using lipoprotein-deficient serum delipidated by the Cab-o-sil method (21), and a time-dependent increase in medium [^{3}H]cholesterol was not observed in the absence of SUVs (data not shown). The current experiments were performed in medium containing serum in which lipoproteins were removed by ultracentrifugation, and [^{3}H]cholesterol does appear in the medium without the addition of SUVs, presumably because of the presence of phospholipids and/or phospholipid/protein acceptors in the serum. Second, we did not observe a time-dependent increase in [^{3}H]cholesteryl ester in the medium, which would have resulted from a secretion of lysosomal contents (data not shown). For these reasons, we think that the source of medium [^{3}H]cholesterol is the plasma membrane.

We have included SUVs in our experiments to provide a

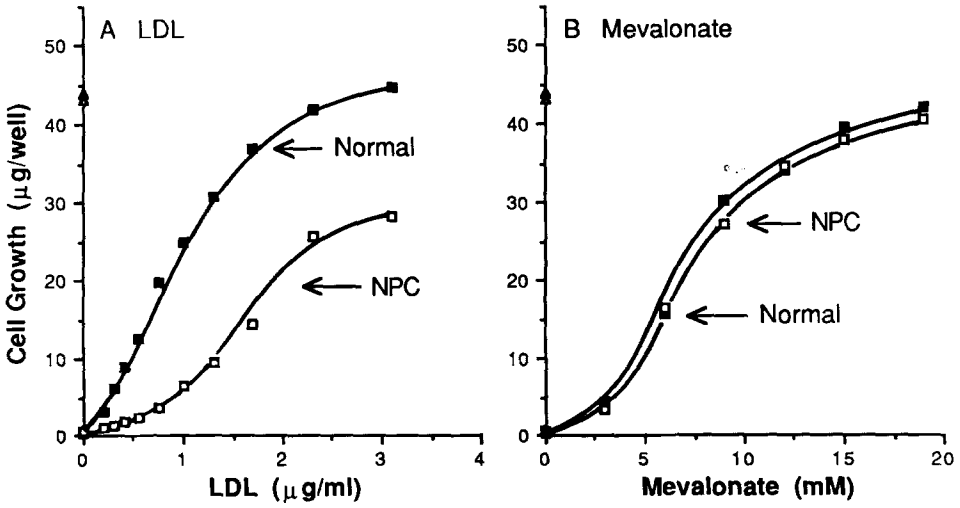

Figure 1. Reversal of mevinolin-inhibited cell growth by LDL (*A*) and mevalonate (*B*) in normal (■) and NPC (□) fibroblasts. Cells were grown according to format 1. On day 1, each monolayer received 1.5 ml of medium B (▲,△) or medium B containing 20 μM mevinolin and 0.15 mM mevalonate plus the indicated concentration of LDL (*A*) or additional mevalonate (*B*) (■,□). On day 8, monolayers were washed, and the protein content of each well was measured as described in Materials and Methods. Each data point represents the average of two wells.

sufficient trap for desorbed cholesterol under all conditions. The SUVs were prepared with a cholesterol/phosphatidylcholine molar ratio similar to that of purified plasma membranes (9) to insure that SUV incubation did not deplete cellular cholesterol levels.

Normal and NPC monolayers were pulsed with [^{3}H-CL]-LDL for 2 h, washed and subjected to chase incubations. Cell-associated [^{3}H]cholesteryl esters, [^{3}H]cholesterol and media [^{3}H]cholesterol were quantitated. Normal and NPC cells pulsed for 2 h with [^{3}H-CL]LDL (0-h chase) contained 26 and 53 nmol/mg of cell-associated [^{3}H]cholesteryl esters, respectively (Fig. 2 *A*). We often found that LDL receptor activity was higher in NPC cells. During the chase, cell-associated [^{3}H]cholesteryl esters were hydrolyzed with the same relative rates in both cell lines. Thus, the amount of cell-associated [^{3}H]cholesterol increased with time proportional to the amount of cellular [^{3}H]cholesteryl esters (Fig. 2 *B*). After 8 h of chase, normal and NPC cells contained 19 and 48 nmol/mg of [^{3}H]cholesterol, respectively.

Although normal cells had a smaller cellular pool of [^{3}H]cholesteryl ester and [^{3}H]cholesterol, the rate at which [^{3}H]cholesterol appeared in the media was faster in normal than in NPC cells. During 8 h of chase, normal and NPC cells desorbed 2.0 and 1.1 nmol/mg of [^{3}H]cholesterol, respectively (Fig. 2 *C*). To correct for differences in the specific activity of the intracellular cholesterol due to increased uptake of [^{3}H-CL]LDL by NPC cells, we expressed the amount of [^{3}H]cholesterol in the media as a percentage of the sum of the cellular [^{3}H]cholesteryl ester plus [^{3}H]cholesterol and medium [^{3}H]cholesterol (Fig. 2 *D*). The data normalized for pool sizes indicates that 8.2% of the LDL-derived [^{3}H]cholesterol in normal cells was desorbed into the medium, while only 1.8% was desorbed from NPC cells during 8 h of chase. These data suggest that LDL-derived [^{3}H]cholesterol is produced equivalently in normal and NPC fibroblasts, but movement of the LDL cholesterol from lysosomes to plasma membranes is less efficient in NPC cells.

We studied the desorption of endogenously synthesized [^{3}H]cholesterol to ascertain whether NPC fibroblasts have a general defect in intracellular cholesterol transport or exhibit defective desorption of plasma membrane cholesterol. Normal and NPC monolayers were pulsed for 2 h with [^{3}H]acetate that is biosynthetically incorporated into cellular [^{3}H]cholesterol, then chased with fresh media. Cellular and media [^{3}H]cholesterol were quantitated. After the 2-h pulse, normal and NPC cells had 270 and 531 pmol/mg of cellular [^{3}H]cholesterol, respectively (Fig. 3 *A*). Similar to the increased LDL receptor activity noted above, a greater rate of cholesterol biosynthesis was evident in NPC cells. The level of cellular [^{3}H]cholesterol remained relatively constant in both cells lines during the chase incubations. [^{3}H]Cholesterol appeared in the media of normal and NPC cells in a time-dependent manner (Fig. 3 *B*). Normal and NPC cells desorbed 249 and 400 pmol/mg of [^{3}H]cholesterol during 8 h of chase, respectively. When the amount of [^{3}H]cholesterol in the medium was expressed as a percentage of the total

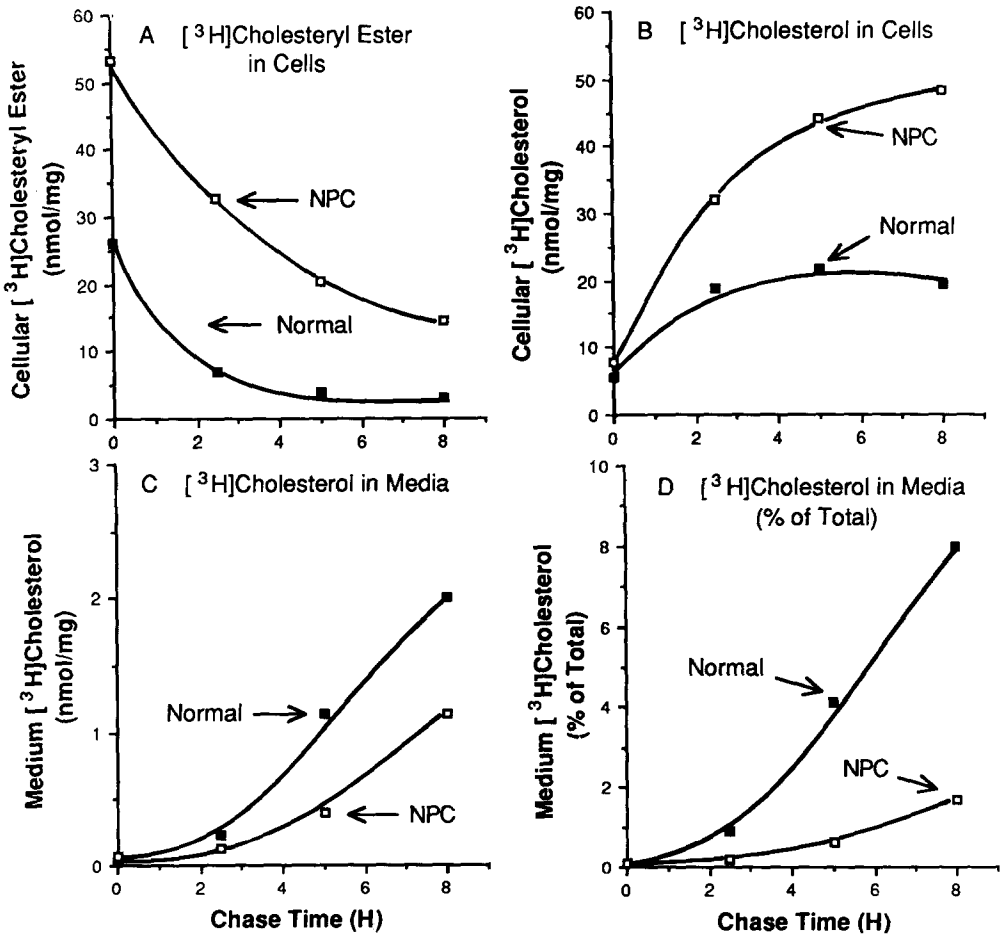

Figure 2. Movement of LDL-derived cholesterol to the plasma membrane in normal (■) and NPC (□) fibroblasts. Cells were grown according to format 2. On day 4, each monolayer received 1 ml of medium C plus 20 μM mevinolin, 1 μg/ml 58-035, and 30 μg/ml [^{3}H-CL]LDL. After 2 h, monolayers were washed and refed with 1 ml of medium C containing 50 μl SUVs. The media were removed after various times, and the cellular [^{3}H]cholesteryl ester (*A*), cellular [^{3}H]cholesterol (*B*), and medium [^{3}H]cholesterol (*C*) contents were determined as described in Materials and Methods. In *D*, the medium [^{3}H]cholesterol is expressed as a percentage of the total cellular [^{3}H]cholesteryl ester and [^{3}H]cholesterol and medium [^{3}H]cholesterol at each time point. Each data point represents the average of three wells.

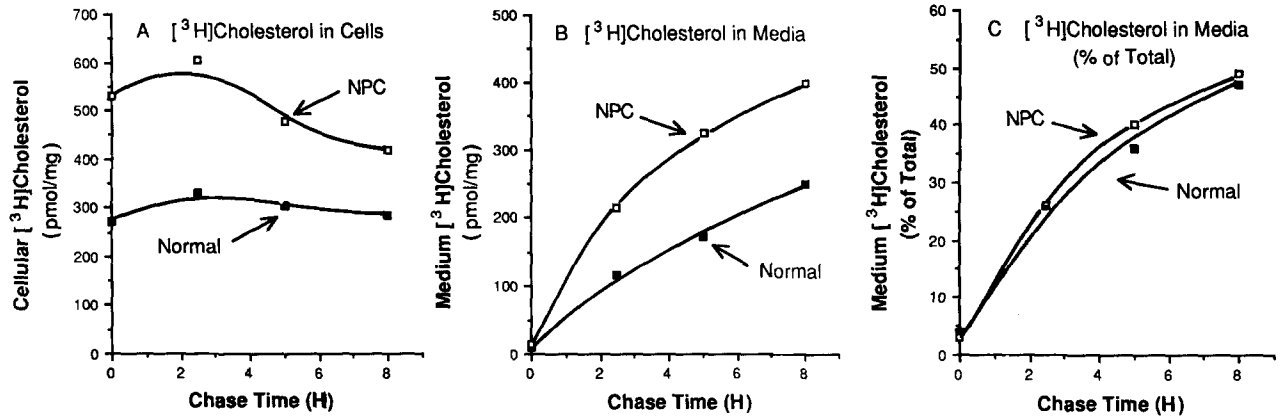

Figure 3. Movement of endogenously synthesized cholesterol to the plasma membrane in normal (■) and NPC (□) fibroblasts. Cells were grown according to format 2 in the same experiment as described in Fig 2. On day 4, each monolayer received 1 ml of medium C plus 15 μCi/ml [^{3}H]acetate. After 2 h, monolayers were washed and refed with 1 ml of medium C containing 50 μl SUVs. The media were removed after various times, and the [^{3}H]cholesterol content of cells (*A*) and media (*B*) were determined as described in Materials and Methods. In *C*, the [^{3}H]cholesterol in the medium is expressed as a percentage of the total cellular [^{3}H]cholesterol and medium [^{3}H]cholesterol at each time point. Each data point represents the average of three wells.

[^{3}H]cholesterol, we observed that the desorption of endogenously synthesized [^{3}H]cholesterol was identical in normal and NPC cells (Fig. 3 *C*).

We observed that the levels of [^{3}H]cholesterol increased substantially in the media, without a corresponding decrease in cellular levels of [^{3}H]cholesterol. This may be because of continued synthesis of [^{3}H]cholesterol during the chase incubation. In subsequent experiments in which mevinolin was included in the chase media, we observed that cellular [^{3}H]cholesterol declined reciprocally with increased media [^{3}H]cholesterol (data not shown).

These transport experiments provide only relative rates of intracellular cholesterol movement for the two fibroblast lines. It is not possible to derive information on the absolute kinetics of intracellular [^{3}H]cholesterol movement using this protocol, because the cholesterol exhange rate between cellular membranes and lipid vesicles is slow compared to the reported transport rates of endogenously derived cholesterol (11, 19). No experiments have reported the intracellular movement of exogenously derived cholesterol. We observed that the rate of appearance of endogenously synthesized [^{3}H]cholesterol in the media was considerably faster than that of LDL-derived [^{3}H]cholesterol. This result may reflect differences in the rate of intracellular movement of cholesterol from its site of synthesis to the plasma membrane versus the movement from the lysosomes to the plasma membrane.

We noted a fourfold difference in the initial rate of appearance of LDL-[^{3}H]cholesterol in the media from normal and NPC cells. This difference gains significance when compared to the identical rate of appearance of acetate-derived [^{3}H]cholesterol in the media of both cell types. The results with endogenously synthesized cholesterol provide an important control for potential differences in the rate of desorption of cholesterol from plasma membranes of normal and NPC cells. That is, if the delayed appearance of LDL-derived [^{3}H]cholesterol in the media of NPC cells was because of impaired desorption of plasma membrane cholesterol, we would expect that the appearance of acetate-derived [^{3}H]cholesterol would also be impaired. As a further control, SUVs containing a nonexchangeable marker, [^{3}H]cholesteryl hexadecyl ether (29), were incubated with monolayers under identical conditions as the above experiment to determine whether SUVs were internalized or fused with the cells. After 8 h of incubation, <1% of the [^{3}H]cholesteryl hexadecyl ether was cell-associated in both normal and NPC cells (data not shown).

We next questioned whether the defective intracellular transport of LDL-derived cholesterol is unique to the NPC phenotype by performing cholesterol desorption experiments (identical to those shown in Figs. 2 and 3) with normal, NPC, and NPA fibroblasts. Once again, we found that LDL-derived [^{3}H]cholesterol appeared threefold slower in the media of NPC compared to normal fibroblasts; however, NPA cells desorbed LDL-derived [^{3}H]cholesterol at the same rate as normal cells (data not shown). [^{3}H]Cholesterol, biosynthetically formed from [^{3}H]acetate, appeared in the media of normal, NPC, and NPA cells with the same time course (data not shown).

Intracellular Movement of LDL-derived Cholesterol in Pulse-labeled Normal and NPC Fibroblasts

We have presented evidence that the movement of LDL-cholesterol from lysosomes to plasma membranes is impaired in NPC fibroblasts. If the movement of LDL-cholesterol is diminished while the rate of LDL-cholesteryl ester hydrolysis is normal, LDL-cholesterol may accumulate at an intracellular site along the transport pathway to the plasma membrane in NPC cells. Is LDL-derived cholesterol accumulating in NPC lysosomes, as was suggested by the fluorescence microscopy studies of Pentchev and co-workers (32)? We used Percoll density gradients to fractionate fibroblast extracts and separate lysosomes from other subcellular organelles, and to follow the time course of movement of LDL-derived [^{3}H]cholesterol within cells.

Normal and NPC fibroblasts were pulsed with [^{3}H-CL]-LDL for 1 h, after which cells were washed and chased in fresh medium for various times. Normal and NPC cells con-

tained 3.4 and 6.1 nmol/mg of cellular [^{3}H]cholesteryl esters after the 1-h pulse, respectively (Fig. 4 *A*). During the chase, the [^{3}H]cholesteryl esters were hydrolyzed, and [^{3}H]-cholesterol accumulated in the cells (Fig. 4 *B*). LDL-derived [^{3}H]cholesterol appeared in the media in a time-dependent manner (Fig. 4 *C*). The chase incubations in this experiment were performed in the absence of SUVs. Nonetheless, the presence of cholesterol acceptors in the serum was sufficient to observe that the appearance of LDL-[^{3}H]cholesterol in the media of NPC cells lagged behind that of normal cells despite the greater content of [^{3}H]cholesterol in NPC cells.

Postnuclear supernatants of cell homogenates were fractionated on Percoll gradients. The distribution of marker enzyme activities in the normal and NPC gradient fractions is shown in Fig. 5. Fig. 5 *A* shows the density profile of a reference Percoll gradient. Fig. 5, *B* and *C*, show the gradient profile of *N*Aβ*G* and 5′ nucleotidase activities, respectively, from extracts of normal and NPC cells harvested at 0-h chase in the experiment depicted in Fig. 4. Approximately 41% and 73% of the *N*Aβ*G* and 5′ nucleotidase activities applied to the gradient was recovered in the gradient fractions (average of 8 experiments). *N*Aβ*G* activity exhibited a bimodal distribution, appearing at the bottom of the gradient (fractions 8–10) as well as the top of the gradient (fractions 1–3). We observed that the *N*Aβ*G* activity sedimenting at the bottom of the gradient was latent (required detergent during the assay), while the *N*Aβ*G* activity at the top of the gradient (fractions 1–3) was not latent and probably represents release of soluble enzyme following lysosomal breakage (data not shown). The majority of the 5′ nucleotidase activity was found in the top fractions of the gradient that we have termed the light membrane fractions. In preliminary experiments, we determined that the light membrane fractions also contain enzyme markers for Golgi complex (galactosyl transferase) and endoplasmic reticulum (3-hydroxy-3-methylglutaryl coenzyme A reductase) (data not shown). A cytosolic marker enzyme, lactate dehydrogenase, was found in fractions 1 and 2 (data not shown).

The distribution of LDL-derived [^{3}H]cholesterol in gradient fractions of normal and NPC fibroblasts after various chase times is shown in Fig. 6. The [^{3}H]cholesterol content of the entire gradient for each chase incubation is shown to emphasize that LDL-[^{3}H]cholesterol was found in the same bimodal distribution in normal and NPC cells; i.e., [^{3}H]cholesterol appears in lysosomes (fractions 9–10) and light membranes (fractions 2–3). Appreciable amounts of [^{3}H]cholesterol are not observed in fraction 1, which contains cytosol.

The time course of appearance of LDL-[^{3}H]cholesterol in gradient fractions revealed marked differences between the two cell lines (Fig. 6). In normal cells, [^{3}H]cholesterol appeared initially (0 h of chase) in the lysosomes and peaked by 2 h. The amount of [^{3}H]cholesterol increased in the light membrane fractions reaching a maximum by 4 h. At 8 h, [^{3}H]cholesterol in the lysosomes had decreased substantially. The [^{3}H]cholesterol content of the light membrane fraction declined as [^{3}H]cholesterol appeared in the media (Fig. 4 *C*). In NPC cells, the LDL-derived [^{3}H]cholesterol content in lysosomes reached a level threefold higher than the level observed in normal lysosomes. During subsequent chase incubations, the appearance of [^{3}H]cholesterol in the light membrane fractions of NPC cells was slower than that observed in normal cells.

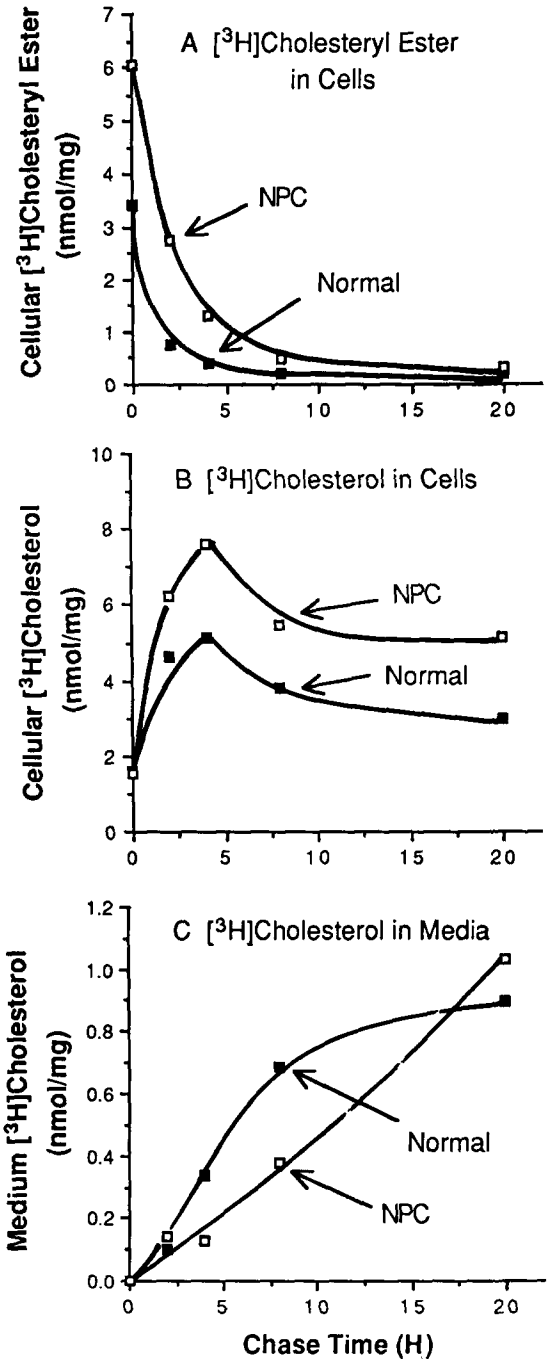

Figure 4. Time course of [^{3}H-CL]LDL metabolism in pulse-labeled normal (■) and NPC (□) fibroblasts. Cells were grown according to format 3. On day 4, monolayers were pulse labeled at staggered times with [^{3}H-CL]LDL (5 μg/ml, 1 h). Monolayers were washed, and chase incubations initiated by the addition of 15 ml of medium C. All dishes were harvested at the same time. Postnuclear supernatants were fractionated on Percoll density gradients as described in Materials and Methods. The analysis of Percoll gradient fractions is illustrated in Figs. 5–7. The content of cellular [^{3}H]cholesteryl ester (*A*), cellular [^{3}H]cholesterol (*B*), and medium [^{3}H]cholesterol (*C*) were determined as described in Cell Fractionation Assays in Materials and Methods. Each data point represents the value from one dish.

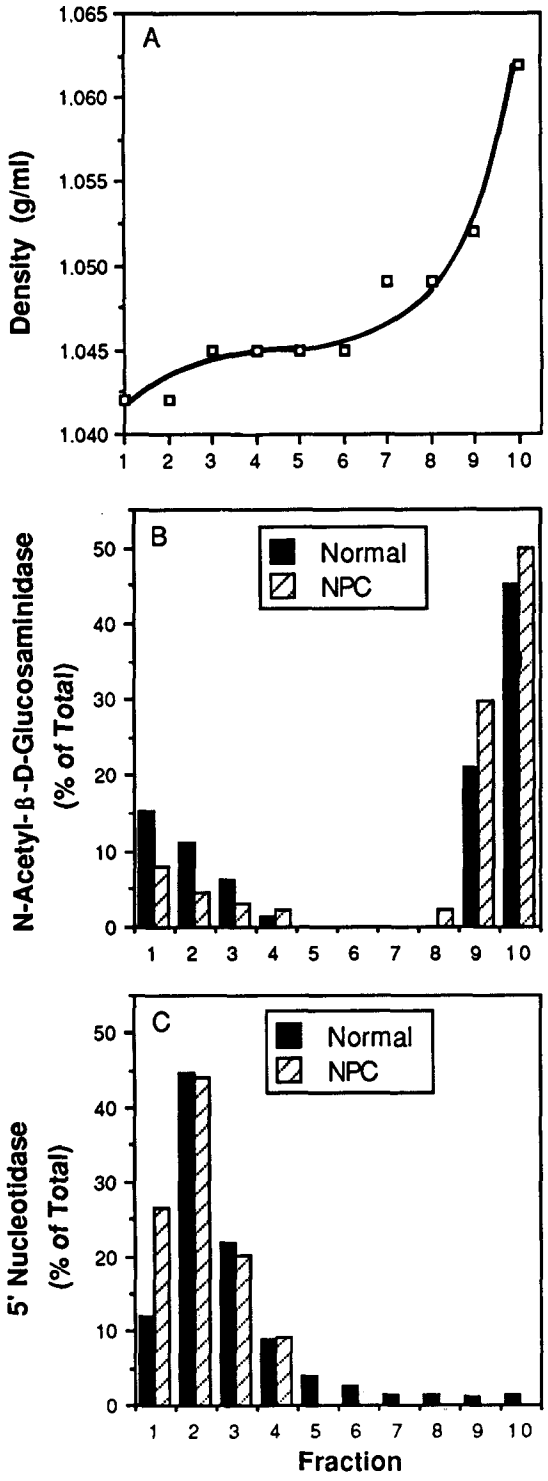

Figure 5. Characterization of Percoll gradient fractions of extracts of normal (■) and NPC (□) fibroblasts. Percoll gradient fractionation of normal (■) and NPC (□) postnuclear supernatants in the experiment described in Fig. 4 was carried out as described in Materials and Methods. *A* shows the density profile of the reference Percoll gradient. *B* shows the distribution of *NAβG* activity in gradient fractions from the 0-h chase normal (■) and NPC (□) extracts. *C* shows the distribution of 5′ nucleotidase activity in gradient fractions from the 0-h chase normal (■) and NPC (□) extracts. Density and enzyme activities were measured as described in Materials and Methods. Enzyme activities are expressed as a percentage of the total enzyme activity in each gradient. Each data point (*A*) or vertical bar (*B* and *C*) represent the value from one gradient fraction.

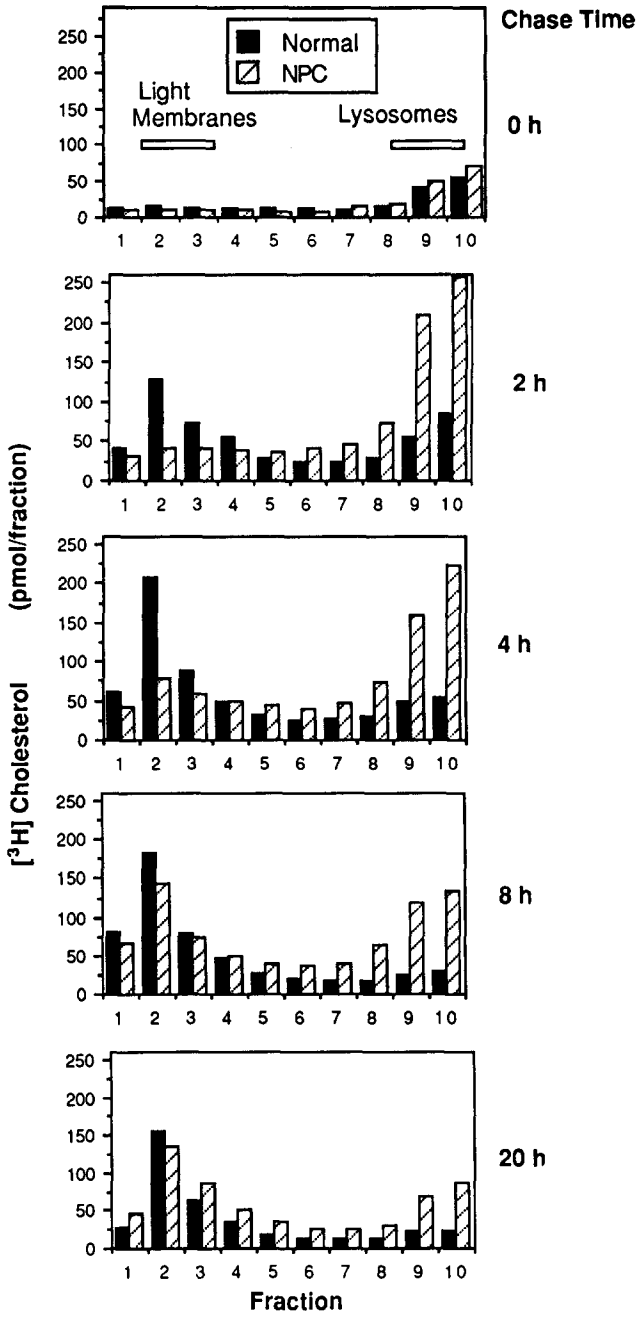

Figure 6. Distribution of [³H]cholesterol in Percoll gradient fractions of pulse-labeled normal (■) and NPC (□) fibroblasts. Percoll gradient fractionation of normal (■) and NPC (□) postnuclear supernatants from the experiment described in Fig. 4 was carried out as described in Materials and Methods. The [³H]cholesterol content of each gradient fraction was determined in Cell Fractionation Assays in Materials and Methods. Each vertical bar represents the value from one gradient fraction.

These data are replotted in Fig. 7 to illustrate the flux of [³H]cholesterol from lysosomes to light membrane fractions. The [³H]cholesterol content of normal and NPC lysosomes (pooled fractions 9–10 from Fig. 6) after various chase times is shown in Fig. 7 *A*. The LDL-[³H]cholesterol content was the same in lysosomes of normal and NPC cells harvested at 0 time. By 2 h of chase, the [³H]cholesterol content of normal lysosomes increased slightly, while the

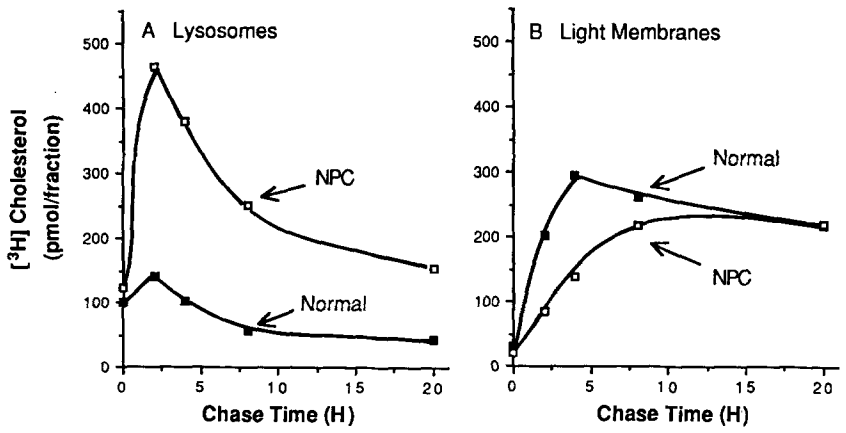

Figure 7. Content of [3H]cholesterol in lysosomal (*A*) and light membrane (*B*) Percoll gradient fractions of pulse-labeled normal (■) and NPC (□) fibroblasts. Percoll gradient fractionation of normal (■) and NPC (□) postnuclear supernatants in the experiment described in Fig. 4 was carried out as described in Materials and Methods. The [3H]cholesterol content of gradient fractions with high *NA*βG activity (fractions 9–10) were summed (*Lysosomes, A*). The [3H]cholesterol content of gradient fractions with high 5′ nucleotidase activity (fractions 2–3) were summed (*Light Membranes, B*). Each data point represents the sum of the [3H]cholesterol in the designated fractions from one gradient.

[3H]cholesterol content of NPC lysosomes increased dramatically to levels threefold higher than normal. [3H]Cholesterol levels then decline in normal and NPC lysosomes with the same apparent rates, reaching half maximal levels after 5 and 6 h, respectively. A much larger fraction of the [3H]cholesterol was retained by the NPC lysosomes. The [3H]cholesterol content of normal and NPC light membranes (pooled fractions 2–3 from Fig. 6) after the chase incubations is shown in Fig. 7 *B*. The [3H]cholesterol content in light membranes of normal cells reached a maximum between 2–4 h of chase, whereas the [3H]cholesterol content of light membranes in NPC cells did not reach a maximum until 8 h of chase.

These data indicate that LDL-derived [3H]cholesterol accumulates to a greater extent in NPC lysosomes (Fig. 7 *A*). Thus, the transfer of LDL-cholesterol to cellular organelles that comprise the light membrane fractions is delayed in NPC cells when compared to normal cells (Fig. 7 *B*). To account for differential homogenization and recovery, we normalized the [3H]cholesterol content of pooled lysosomes and light membranes for units of *NA*βG and 5′ nucleotidase enzyme activities, respectively, and for protein content in the postnuclear supernatants. The results were qualitatively the same as those illustrated in Fig. 7; i.e., LDL-cholesterol accumulated to a greater extent in lysosomes and was delayed in movement to other membranes of NPC cells (data not shown).

Intracellular Movement of LDL-derived Cholesterol in Continuously Labeled Normal and NPC Fibroblasts

The steady-state accumulation of LDL-derived [3H]cholesterol in normal and NPC lysosomes was revealed when cells were continuously labeled with [3H-CL]LDL and processed as described above in the pulse–chase experiment.

Normal and NPC cells exhibited a similar time-dependent increase in total cellular [3H]cholesterol content (Fig. 8 *A*). [3H]Cholesterol levels in lysosomes increased with the same initial rate, and reached steady-state levels that were 2.5-fold higher in NPC than normal lysosomes (Fig. 8 *B*). The data suggest that levels of lysosomal [3H]cholesterol reached steady state at ~8 h in both cell types. The appearance of [3H]cholesterol in light membrane fractions was delayed in NPC cells as compared to normal cells (Fig. 8 *C*). However, after a 4-h lag, the rate of appearance of [3H]cholesterol in light membranes was comparable in normal and NPC cells.

The results of the pulse chase and continuous label experiments concur with the observation that LDL-derived cholesterol accumulates in NPC lysosomes and that the initial movement of LDL-derived cholesterol to other cellular membranes is delayed in NPC fibroblasts.

LDL-induced Increase in Cholesterol Content in Normal and NPC Subcellular Fractions

Normal and NPC monolayers were incubated in the absence or presence of 25 μg/ml LDL for 14 h, after which the cells were washed, harvested, and homogenized. Postnuclear supernatants were fractionated on Percoll gradients to separate lysosomes from light membranes. Aliquots of postnuclear supernatants, light membrane, and lysosomal fractions were analyzed for cholesterol and protein content and marker enzyme activities. Cholesterol content in light membranes and lysosomes was normalized for 5′ nucleotidase and *NA*βG activities, respectively, to account for recovery of membranes from the Percoll fractions. These data are shown in Table I.

The cholesterol content of postnuclear supernatants derived from normal and NPC cells cultured in the absence of LDL was identical. As previously reported (27), NPC fibroblasts accumulated more unesterified cholesterol when incubated with LDL. LDL induced a 2.2- and 3.6-fold increase in the cholesterol content of normal and NPC postnuclear supernatants, respectively. The LDL-induced overaccumulation of cholesterol in NPC cells was not apparent in the cholesterol content of the light membrane fractions. LDL incubation caused a similar increase in light membrane cholesterol for both normal and NPC cells. The cholesterol content of lysosomes from normal and NPC cells cultured in the absence of LDL was not significantly different; however, a striking difference was seen in the lysosomal cholesterol content of cells incubated in the presence of LDL. When incubated with LDL, NPC fibroblasts accumulated three times more cholesterol in lysosomes compared to normal cells.

Discussion

NPC disease is characterized by a substantial intracellular accumulation of unesterified cholesterol (6). We and Pentchev and colleagues have sought to explain the accumulation of unesterified cholesterol in NPC cells. We have found that LDL binding and internalization (21, 26), and lysosomal hydrolysis of LDL-cholesteryl esters (21) are normal in NPC cells. However, LDL does not stimulate cholesterol es-

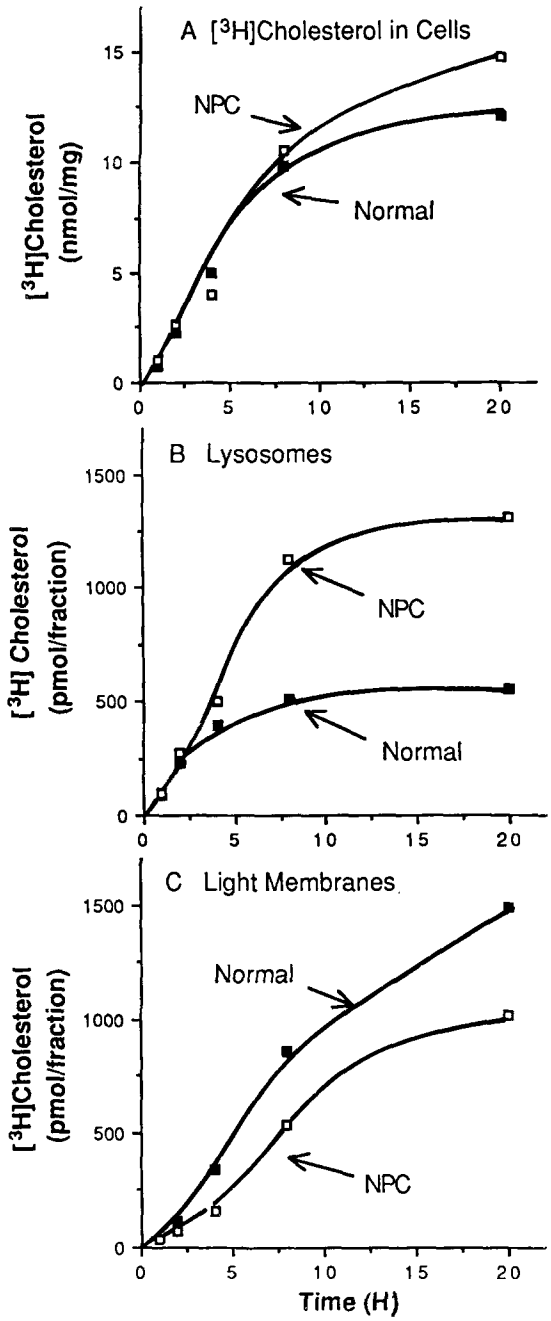

Figure 8. Cellular [^{3}H]cholesterol content (*A*) and content of [^{3}H]cholesterol in lysosomal (*B*) and light membrane (*C*) Percoll gradient fractions of continuously labeled normal (■) and NPC (□) fibroblasts. Cells were grown according to format 3. On day 5, monolayers were pulsed at staggered times with [^{3}H-CL]LDL (2 μg/ml). All dishes were harvested at the same time. Percoll gradient fractionation of normal (■) and NPC (□) postnuclear supernatants was carried out as described in Materials and Methods. The content of cellular [^{3}H]cholesterol (*A*) was determined as described in Cell Fractionation Assays in Materials and Methods. Each data point represents the value of one dish. The [^{3}H]cholesterol content of gradient fractions with high *N*Aβ*G* activity (fractions 8–10) were summed (*Lysosomes, B*). The [^{3}H]cholesterol content of gradient fractions with high 5′ nucleotidase activity (fractions 2–4) were summed (*Light Membranes, C*). Each data point represents the sum of the [^{3}H]cholesterol in the designated fractions from one gradient.

terification in NPC cells (21, 25). Although LDL does mediate suppression of cellular cholesterol synthesis and LDL receptor activity, these responses occur only after a prolonged time lag in NPC cells (21, 27). The accumulation of unesterified cholesterol in NPC cells cultured with LDL appears to result from an inability of LDL to stimulate cholesterol esterification in addition to the lag in LDL-mediated down regulation of LDL receptor activity and cellular cholesterol synthesis. The defect in NPC appears to be specific for LDL, since nonlipoprotein effectors, such as 25-hydroxycholesterol and mevalonate, do elicit normal regulatory responses in NPC cells (21). However, the defective regulation may also extend to other sources of exogenous cholesterol which may enter cells via a lysosomal pathway (25).

There are several possible explanations for impaired LDL-mediated regulation of cholesterol metabolism in NPC cells. First, the transport of LDL-derived cholesterol from lysosomes to intracellular regulatory sites may be defective. Second, LDL-derived cholesterol might normally regulate cellular cholesterol metabolism by further metabolism of the unesterified cholesterol to a regulatory sterol. The NPC mutation may prevent the metabolic conversion of LDL-derived cholesterol to this putative regulatory sterol. Third, LDL-derived cholesterol may regulate cellular cholesterol metabolism via a second messenger, which may be compromised in NPC cells.

Four lines of evidence indicate that NPC cells express a defect in intracellular transport of LDL-derived cholesterol. First, we find that mevinolin-inhibited NPC cells are inefficient in using LDL-cholesterol for growth. However, exogenously added mevalonate restores cell growth equally in normal and NPC cells. Thus, the inability of cholesterol to fulfill growth requirements in NPC cells is restricted to LDL-derived cholesterol. This may reflect impaired movement of LDL-derived cholesterol from lysosomes to cell membranes. Although recent progress has been made in elucidating the kinetics and mechanism of movement of newly synthesized cholesterol from the endoplasmic reticulum to the plasma membrane (17, 19, 20), the mechanism and pathway of intracellular transport of LDL-cholesterol remains unknown.

Second, we determined the relative rate of movement of LDL-cholesterol to the plasma membrane in normal and NPC cells by measuring the amount of LDL-derived [^{3}H]-cholesterol that appears in the media. The results indicate that LDL-derived cholesterol is transported to the plasma membrane slower in NPC than in normal cells. NPC cells do not exhibit a general defect in intracellular cholesterol transport since [^{3}H]acetate-derived cholesterol desorbs normally in NPC cells. In addition, mevalonate-derived cholesterol fulfills growth requirements normally in NPC cells. Third, subcellular fractionation of [^{3}H-CL]LDL-labeled cells shows that, in NPC cells, LDL-cholesterol accumulates to higher levels in lysosomes and its movement to other cell membranes is delayed.

Fourth, cholesterol content data was needed to resolve whether the retention of LDL-cholesterol in NPC lysosomes was due to either a smaller cholesterol pool in lysosomes of NPC cells grown in lipoprotein-deficient serum-containing media, or to defective transport of LDL-cholesterol from NPC lysosomes. The data in Table I indicate that the latter may explain LDL-cholesterol retention in NPC lysosomes. We find that the cholesterol content of normal and NPC lyso-

somes are equivalent when cells are cultured in lipoprotein-deficient serum. However, incubation with LDL invokes a much greater increase in cholesterol mass in NPC lysosomes.

The cholesterol transport studies are consistent with the biochemical analyses that reveal a delayed time course of LDL-mediated regulation of cholesterol synthesis and LDL receptor activity in NPC cells (21, 27). That is, in NPC cells, the impaired movement of LDL-cholesterol may explain the extended time lag seen in LDL-mediated regulation of these two activities. However, the cholesterol transport studies are inconsistent with the decided block in the ability of LDL to stimulate cholesterol esterification (21, 25). Impaired lipoprotein-mediated regulation of cellular cholesterol metabolism was also reported by Tabas et al. (33–35) in comparative studies using two macrophage cell lines incubated with native or modified LDL. Tabas' results suggest that macrophage cell lines may employ different cholesterol transport routes depending on the lipoprotein source.

As predicted from earlier studies on LDL metabolism (for review, see reference 8), we note that unesterified, LDL-derived cholesterol initially appears in lysosomes. During continuous exposure to LDL, the lysosomal content of LDL-cholesterol plateaus coincident with the initial appearance of LDL-cholesterol in the light membrane fractions. The plateau is indicative of a steady state in which the production of unesterified cholesterol in the lysosomes (by continual receptor-mediated endocytosis and hydrolysis of LDL) is balanced by the movement of LDL-cholesterol out of the lysosomes. We believe that the use of [^{3}H-CL]LDL and subcellular fractionation will prove useful in studying LDL-cholesterol movement in a variety of systems.

Evidence of cholesterol overaccumulation in NPC lysosomes was first indicated by fluorescence microscopy. Kruth et al. (18) used filipin to detect unesterified cholesterol in normal and NPC fibroblasts. In NPC cells incubated with LDL, unesterified cholesterol was found to accumulate within spherical inclusions with a perinuclear distribution similar to that of lysosomes. In a later study, filipin staining of LDL-incubated NPC cells was shown to colocalize with indirect immunochemical staining of a lysosomal membrane protein (32). These studies did not discern the source of cholesterol accumulating in lysosomes of LDL-incubated cells.

Pentchev and coworkers also used Percoll gradients to determine the site of cholesterol accumulation in NPC fibroblasts cultured with LDL (27). They found that, in normal and NPC cells incubated in the absence of LDL, unesterified cholesterol mass colocalized with light membranes that contained plasma membrane and Golgi complex marker enzymes. Incubation with 50 μg/ml LDL for 48 h did not alter the cholesterol distribution in normal or NPC cells. However, in LDL-incubated NPC cells, there was a substantial redistribution of the lysosomal marker enzyme that now largely colocalized with cholesterol-containing, light membrane fractions. These "light lysosomes" may be the consequence of prolonged incubation of NPC cells with high concentrations of LDL. An excessive accumulation of cholesterol in NPC lysosomes could result in decreased buoyant density of the organelle. We do not observe a density shift in lysosomal enzyme activity in NPC cells incubated with LDL for two possible reasons. First, we incubated cells with a relatively low concentration of LDL (10–25 μg/ml) for short incubation periods (1–20 h). These milder conditions were similar to those used for the LDL-mediated regulation studies of normal and NPC cells (21). Second, our Percoll gradients were formed using a lower Percoll starting density. In our hands, the higher concentrations of Percoll that are routinely used to isolate lysosomes (23, 31) did not separate lysosomes from other subcellular organelles. Consequently, our Percoll gradients may not separate light and heavy lysosomes. Pentchev concluded that, in NPC cells, LDL incubation causes excess unesterified sterol to accumulate in the light lysosome–light membrane region of the Percoll gradient (27). In our experiments, we are able to differentiate between lysosomes and light membranes. Most importantly, the use of [^{3}H-CL]LDL allows us to measure the accumulation of LDL-[^{3}H]cholesterol, specifically, in NPC lysosomes.

A defect in cholesterol transport in NPC cells was also deduced from experiments that utilized cholesterol oxidase to measure levels of plasma membrane cholesterol (32). This report did not address whether the defect encompassed the transport of newly synthesized and/or LDL-derived cholesterol. Our results complement those of Sokol et al. (32) and extend the observation to show that endogenously synthesized cholesterol is transported normally, while LDL-cholesterol transport is defective in NPC cells.

Blanchette-Mackie et al. (4) have recently shown, using cytochemical techniques, that NPC cells incubated with LDL also accumulate cholesterol in the Golgi complex. They suggest that components of the Golgi complex may play a role in the intracellular movement of exogenously derived cholesterol, and that impairment of cholesterol movement in the Golgi complex may be partly responsible for the defect seen in NPC cells. If cholesterol trafficking in the Golgi complex is disrupted in NPC cells, one may expect to see impaired movement of endogenously derived cholesterol. Yet, our results indicate that endogenously derived cholesterol moves normally in NPC cells. Even if LDL-cholesterol transport is impaired in the Golgi complex of NPC cells, our results could be explained if endogenously synthesized cholesterol is not transported through the Golgi complex, or if endogenously synthesized and LDL-derived cholesterol assume different routes through the Golgi complex stacks.

The defect in intracellular cholesterol transport appears to be specific for NPC. Experiments to measure the appearance of LDL-[^{3}H]cholesterol in the media, as described in Figs. 2 and 3, were also conducted with NPA fibroblasts. NPA cells, exhibiting no detectable lysosomal sphingomyelinase activity, were chosen to determine if high lysosomal sphingomyelin levels could be responsible for the impaired cholesterol transport seen in NPC cells. Sphingomyelin has a higher affinity than other phospholipids for cholesterol (28), and in vitro experiments have shown that cholesterol preferentially partitions into sphingomyelin-containing bilayers (28). Nonetheless, we observed that LDL-derived [^{3}H]cholesterol was transported from lysosomes to plasma membranes normally in NPA cells (data not shown). This result indicates that the accumulation of LDL-cholesterol in NPC lysosomes, and the delayed movement of LDL-cholesterol to the plasma membrane, is not a result of coaccumulation of sphingomyelin in NPC lysosomes. This finding is consistent with the report of Pentchev et al. (25) that LDL-stimulated cholesterol esterification is normal in NPA cells.

What causes the accumulation of LDL-derived cholesterol

in NPC lysosomes? First, cholesterol may be retained in lysosomes because of the presence of either a unique protein or lipid, or aberrant levels of a normal lysosomal protein or lipid. A lysosomal component with the potential to affect cholesterol movement is sphingomyelin; however, it is unlikely that excess sphingomyelin is the cause, since LDL-cholesterol transport is normal in NPA cells. Once the higher cholesterol level is reached in NPC lysosomes, cholesterol appears to leave NPC and normal lysosomes with similar rates (see Figs. 7 *A* and 8 *B*). This raises the possibility that cholesterol must fill a larger pool in NPC lysosomes, after which the rate of exit is normal. The regulation studies (21, 27) also show that NPC cells exhibit a prolonged lag phase beyond which LDL-mediated suppression of cholesterol synthesis and LDL receptor activity proceeds with normal time courses. Alternatively, NPC cells may be expressing defective extralysosomal components, such as carrier proteins or lipids, or specific vesicular/micellar elements that may mediate intracellular cholesterol transport.

O. J. Murphy III provided excellent technical assistance. We thank E. Dawidowicz for many helpful discussions, for critically reading the manuscript, and for the use of his gas chromatograph. We thank M. Krieger and J. F. Dice for critically reviewing the manuscript.

This work was supported by grants from the National Institutes of Health (DK 36505) and by the Center for Gastroenterology Research on Absorptive and Secretory Processes (AM 39428). L. Liscum is an Established Investigator of the American Heart Association. R. Ruggiero is the recipient of a postdoctoral fellowship from the American Heart Association, Massachusetts affiliate. J. Faust is supported by a National Institutes of Health Training Grant (DK 07542).

Received for publication 15 November 1988 and in revised form 9 January 1989.

References

1. Ames, B. N. 1966. Assay of inorganic phosphate, total phosphate and phosphatases. *Methods Enzymol.* 8:115–118.
2. Backer, J. M., and E. A. Dawidowicz. 1979. The rapid transmembrane movement of cholesterol in small unilamellar vesicles. *Biochim. Biophys. Acta.* 551:260–270.
3. Barrett, A. J. 1972. Lysosomal enzymes. *In* Lysosomes: a laboratory handbook. J. T. Dingle, editor. North-Holland Publishing Co., Amsterdam. 46–135.
4. Blanchette-Mackie, E. J., N. K. Dwyer, L. M. Amende, H. S. Kruth, J. D. Butler, J. Sokol, M. E. Comly, M. T. Vanier, J. T. August, R. O. Brady, and P. G. Pentchev. 1988. Type-C Niemann-Pick disease: low density lipoprotein uptake is associated with premature cholesterol accumulation in the Golgi complex and excessive cholesterol storage in lysosomes. *Proc. Natl. Acad. Sci. USA.* 85:8022–8026.
5. Bligh, E. G., and W. J. Dyer. 1959. A rapid method of total lipid extraction and purification. *Can. J. Biochem. Physiol.* 37:911–917.
6. Brady, R. O. 1983. Sphingomyelin lipidoses: Niemann-Pick disease. *In* The Metabolic Basis of Inherited Disease. 5th ed. J. B. Stanbury, J. B. Wyngaarden, D. S. Fredrickson, J. L. Goldstein, and M. S. Brown, editors. McGraw-Hill Publications, Minneapolis, MN. 831–841.
7. Brown, M. S., and J. L. Goldstein. 1980. Multivalent feedback regulation of HMG CoA reductase, a control mechanism coordinating isoprenoid synthesis and cell growth. *J. Lipid Res.* 21:505–517.
8. Brown, M. S., and J. L. Goldstein, 1986. A receptor-mediated pathway for cholesterol homeostasis. *Science (Wash. DC).* 232:34–47.
9. Colbeau, A., J. Nachbaur, and P. M. Vignais. 1971. Enzymic characterization and lipid composition of rat liver subcellular membranes. *Biochim. Biophys. Acta.* 249:462–492.
10. Dawidowicz, E. A. 1987. Dynamics of membrane lipid metabolism and turnover. *Annu. Rev. Biochem.* 56:43–61.
11. DeGrella, R. F., and R. D. Simoni. 1982. Intracellular transport of cholesterol to the plasma membrane. *J. Biol. Chem.* 257:14256–14262.
12. Faust, J. R., M. S. Brown, and J. L. Goldstein. 1980. Synthesis of Δ^2-isopentenyl tRNA from mevalonate in cultured human fibroblasts. *J. Biol. Chem.* 255:6546–6548.
13. Faust, J. R., J. L. Goldstein, and M. S. Brown. 1977. Receptor-mediated uptake of low density lipoprotein and utilization of its cholesterol for steroid synthesis in cultured mouse adrenal cells. *J. Biol. Chem.* 252:4861–4871.
14. Faust, J. R., J. L. Goldstein, and M. S. Brown. 1979. Synthesis of ubiquinone and cholesterol in human fibroblasts: regulation of a branched pathway. *Arch. Biochem. Biophys.* 192:86–99.
15. Folch, J., M. Lees, and G. H. Sloane Stanley. 1957. A simple method for the isolation and purification of total lipids from animal tissues. *J. Biol. Chem.* 226:497–509.
16. Goldstein, J. L., S. K. Basu, and M. S. Brown. 1983. Receptor-mediated endocytosis of low-density lipoprotein in cultured cells. *Methods Enzymol.* 98:241–260.
17. Kaplan, M. R., and R. D. Simoni. 1985. Transport of cholesterol from the endoplasmic reticulum to the plasma membrane. *J. Cell Biol.* 101:446–453.
18. Kruth, H. S., M. E. Comly, J. D. Butler, M. T. Vanier, J. K. Fink, D. A. Wenger, S. Patel, and P. G. Pentchev. 1986. Type C Niemann-Pick disease. Abnormal metabolism of low density lipoprotein in homozygous and heterozygous fibroblasts. *J. Biol. Chem.* 261:16769–16774.
19. Lange, Y., and H. J. G. Matthies. 1984. Transfer of cholesterol from its site of synthesis to the plasma membrane. *J. Biol. Chem.* 259:14624–14630.
20. Lange, Y., and T. L. Steck. 1985. Cholesterol-rich intracellular membranes: a precursor to the plasma membrane. *J. Biol. Chem.* 260:15592–15597.
21. Liscum, L., and J. R. Faust. 1987. Low density lipoprotein (LDL)-mediated suppression of cholesterol synthesis and LDL uptake is defective in Niemann-Pick type C fibroblasts. *J. Biol. Chem.* 262:17002–17008.
22. Lowry, O. H., N. J. Rosebrough, A. L. Farr, and R. J. Randall. 1951. Protein measurement with the Folin phenol reagent. *J. Biol. Chem.* 193: 265–275.
23. McElligott, M. A., P. Miao, and J. F. Dice. 1985. Lysosomal degradation of ribonuclease A and ribonuclease S-protein microinjected into the cytosol of human fibroblasts. *J. Biol. Chem.* 260:11986–11993.
24. Mosley, S. T., M. S. Brown, R. G. W. Anderson, and J. L. Goldstein. 1983. Mutant clone of Chinese hamster ovary cells lacking 3-hydroxy-3-methylglutaryl coenzyme A reductase. *J. Biol. Chem.* 258:13875–13881.
25. Pentchev, P. G., M. E. Comly, H. S. Kruth, M. T. Vanier, D. A. Wenger, S. Patel, and R. O. Brady. 1985. A defect in cholesterol esterification in Niemann-Pick disease (type C) patients. *Proc. Natl. Acad. Sci. USA.* 82: 8247–8251.
26. Pentchev, P. G., H. S. Kruth, M. E. Comly, J. D. Butler, M. T. Vanier, D. A. Wenger, and S. Patel. 1986. Type C Niemann-Pick disease. A parallel loss of regulatory responses in both the uptake and esterification of low density lipoprotein-derived cholesterol in cultured fibroblasts. *J. Biol. Chem.* 261:16775–16780.
27. Pentchev, P. G., M. E. Comly, H. S. Kruth, T. Tokoro, J. Butler, J. Sokol, M. Filling-Katz, J. M. Quirk, D. C. Marshall, S. Patel, M. T. Vanier, and R. O. Brady. 1987. Group C Niemann-Pick disease: faulty regulation of low-density lipoprotein uptake and cholesterol storage in cultured fibroblasts. *FASEB (Fed. Am. Soc. Exp. Biol.) J.* 1:40–45.
28. Phillips, M. C., W. J. Johnson, and G. H. Rothblat. 1987. Mechanisms and consequences of cellular cholesterol exchange and transfer. *Biochim. Biophys. Acta.* 906:223–276.
29. Pool, G. L., M. E. French, R. A. Edwards, L. Huang, and R. H. Lumb. 1982. Use of radiolabeled hexadecyl cholesteryl ether as a liposome marker. *Lipids.* 17:448–452.
30. Poznansky, M. J., and S. Czekanski. 1982. Cholesterol movement between human skin fibroblasts and phosphatidylcholine vesicles. *Biochim. Biophys. Acta.* 685:182–190.
31. Rome, L. H., A. J. Garvin, M. M. Allietta, and E. F. Neufeld. 1979. Two species of lysosomal organelles in cultured human fibroblasts. *Cell.* 17: 143–153.
32. Sokol, J., J. Blanchette-Mackie, H. S. Kruth, N. K. Dwyer, L. M. Amende, J. D. Butler, E. Robinson, S. Patel, R. O. Brady, M. E. Comly, M. T. Vanier, and P. G. Pentchev. 1988. Type C Niemann-Pick disease. Lysosomal accumulation and defective intracellular mobilization of low density lipoprotein cholesterol. *J. Biol. Chem.* 263:3411–3417.
33. Tabas, I., D. A. Weiland, and A. R. Tall. 1985. Unmodified low density lipoprotein causes cholesteryl ester accumulation in J774 macrophages. *Proc. Natl. Acad. Sci. USA.* 82:416–420.
34. Tabas, I., D. A. Weiland, and A. R. Tall. 1986. Inhibition of acyl coenzyme A:cholesterol acyl transferase in J774 macrophages enhances down-regulation of the low density lipoprotein receptor and 3-hydroxy-3-methylglutaryl-coenzyme A reductase and prevents low density lipoprotein-induced cholesterol accumulation. *J. Biol. Chem.* 261:3147–3155.
35. Tabas, I., G. C. Boykow, and A. R. Tall. 1987. Foam cell-forming J774 macrophages have markedly elevated acyl coenzyme A/cholesterol acyl transferase activity compared with mouse peritoneal macrophages in the presence of low density lipoprotein (LDL) despite similar LDL receptor activity. *J. Clin. Invest.* 79:418–426.
36. Widnell, C. C. 1974. Purification of rat liver 5'-nucleotidase as a complex with sphingomyelin. *Methods Enzymol.* 32:368–374.